Effective Field Theory in quest to parametrise Higgs properties: the transverse momentum spectrum case

2017 J. Phys.: Conf. Ser. 873 012050

(http://iopscience.iop.org/1742-6596/873/1/012050)

IOP Conf. Series: Journal of Physics: Conf. Series **873** (2017) 012050 doi:10.1088/1742-6596/873/1/012050

Effective Field Theory in quest to parametrise Higgs properties: the transverse momentum spectrum case

Massimiliano Grazzini[a], **Agnieszka Ilnicka**[abc], **Michael Spira**[c], **Marius Wiesemann**[d]

[a] Physics Institute, University of Zürich, Winterthurerstrasse 190, CH-8057 Zürich
[b] Physics Department, ETH Zürich, Otto-Stern-Weg 5, CH-8093 Zürich
[c] Paul Scherrer Institute, CH-5232 Villigen PSI
[d] CERN Theory Division, CH-1211, Geneva 23

E-mail: grazzini@physik.uzh.ch, ailnicka@physik.uzh.ch, michael.spira@psi.ch, marius.wiesemann@cern.ch

Abstract. After the Higgs boson discovery, LHC turned into the precision machine to explore its properties. In case new resonances will not be found, the only access to New Physics would be via measuring small deviations from the SM predictions. A consistent approach which can be useful in both above cases is a bottom-up Effective Field Theory, with dimension six operators build of Standard Model fields. We present how this approach would work in case of the transverse momentum spectrum of the Higgs particle. In our calculation we augmented the Standard Model with three additional operators: modifications of the top and bottom Yukawa couplings, and a point-like Higgs coupling to gluons. We present resummed transverse-momentum spectra including the effect of these operators at NLL+NLO accuracy and study their impact on the shape of the distribution. We find that such modifications, while affecting the total rate within the current uncertainties, can lead to significant distortions of the spectrum. We also discuss the effect of the chromomagnetic operator on the Higgs production cross section at LO.
For more details see our paper [1].

1. Introduction

The scalar resonance discovered by ATLAS and CMS at the LHC in 2012 [2, 3] closely resembles the Higgs boson postulated in the Standard Model (SM). The SM, however, is not able to explain the existence of dark matter, the matter-antimatter asymmetry and the relatively low scale of electroweak symmetry breaking (hierarchy problem). Many theories beyond the SM (BSM) addressing the above issues have been developed, which manifest different patterns in the scalar sector and in the Higgs boson properties. As no strict argument exists for the discovery of new physics at the TeV scale, it is possible that new physics effects are accessible only by measuring small deviations from SM predictions. A consistent way to parametrise these deviations is offered by the Effective Field Theory (EFT), in which the unknown high-scale fields are integrated out leaving an infinite ladder of higher-dimensional operators (dim$>$ 4), with a well-defined hierarchy. The EFT can thus be used to build a bottom-up approach in which the usual dimension-four operators in the SM are augmented by leading (dimension-six) operators. Experimental data can be employed to fix the values of the so-called Wilson coefficients of these

operators. A matching to the EFT allows then for the translation of the Wilson coefficients into bounds on the physical parameters of new physics models. The full set of dimension-six [4, 5] deformations of the SM was classified by 59 operators. The precision observables measured at LEP and the Tevatron put bounds on many of the Wilson coefficients, some even at the per-mille level [6, 7, 8]. However, several operators involving the Higgs field are still essentially unbounded. In the following, we therefore develop a strategy to determine such bounds by using the transverse-momentum (p_T) spectrum of the Higgs boson.

2. Transverse-momentum spectrum

Kinematical distributions provide an important handle on the determination of Higgs properties. Among the most important observables in this respect is the Higgs transverse-momentum distribution, that will be measured with high precision in Run II and High Luminosity stage of the LHC. First results from the LHC Run I were presented by the ATLAS collaboration in the 2γ and four-lepton final states [9, 10] and by the CMS collaboration in the 2γ final state [11], leaving still a significant amount of arbitrariness for the precise form of the distribution. The p_T spectrum provides more information than the total cross section, which is just one number; the shape, the position of the maximum and the normalisation allow us to disentangle effects that remain hidden in the total rates. For example, it is the simplest measurement to shed light on the nature of the Higgs coupling to gluons. The fact that the Higgs is a scalar, gives an additional simplification in the modeling of the Higgs p_T-spectrum, due to the factorization of production and decay in the narrow-width approximation.

The most important Higgs production channel at the LHC is gluon fusion, which, despite being a loop-induced process, is highly enhanced by the dominance of the gluon densities [12]. Therefore, we will concentrate on the spectra obtained in this production channel. In the past years a significant amount of work has been done to improve the precision of the calculations of the Higgs p_T spectrum. The first results at the lowest order ($\mathcal{O}(\alpha_S^3)$) were known since long time [13, 14]. It took nearly ten years until the $\mathcal{O}(\alpha_S^4)$ corrections were computed [15, 16, 17, 18]. These were carried out in the heavy-top limit (HTL, i.e. $m_t^2 \gg M_H^2, p_{TH}^2$).[1] Recently, results on Higgs+jet production at $\mathcal{O}(\alpha_S^5)$ were also obtained in HTL [21, 22, 23].

In the low-p_T region ($p_T \ll M_H$), the perturbative expansion is affected by large logarithmic terms of the form $\alpha_S^n \ln^m(m_H^2/p_T^2)$, with $1 \leq m \leq 2n$. This results in a singular behaviour of the distribution as $p_T \to 0$. To cure this problem one needs to resum these terms to all orders in α_S [24]. The resummation is carried out in impact parameter (b) space, and, in particular, we use the formalism of Ref. [25]. The resummed and fixed order results have to be properly matched at intermediate p_T to avoid double counting:

$$\left[\frac{\mathrm{d}\sigma}{\mathrm{d}p_T^2}\right]_{\text{f.o.+a.o.}} = \left[\frac{\mathrm{d}\sigma}{\mathrm{d}p_T^2}\right]_{\text{f.o.}} - \left[\frac{\mathrm{d}\sigma^{(\text{res})}}{\mathrm{d}p_T^2}\right]_{\text{f.o.}} + \left[\frac{\mathrm{d}\sigma^{(\text{res})}}{\mathrm{d}p_T^2}\right]_{\text{a.o.}} \tag{1}$$

where f.o. corresponds to fixed order, and a.o. to all orders calculations. In the formalism of Ref. [25], a unitarity constraint is enforced, such that the integral of the p_T-spectrum coincides with the corresponding total inclusive cross section computed at fixed order. More precisely, by performing the resummation at next-to-leading logarithmic accuracy (NLL) and including the fixed order result up to $O(\alpha_S^3)$ we obtain NLO+NLL accuracy, and the integral of the spectrum is fixed to the NLO total cross section. Top-and bottom-mass effects can be included in the resummed spectrum along the lines of Refs. [26, 27].

The inclusion of dimension-six and dimension-eight operators in the p_T-spectrum has been considered in Refs. [28, 29, 30, 31] and [32, 33], respectively. Strategies for extracting information

[1] Finite top-mass effects on the Higgs p_T distribution at $\mathcal{O}(\alpha_S^4)$ were estimated in Refs. [19, 20].

on the Higgs-gluon couplings from the measurements were studied in Ref. [30]. Most of the above studies, however, are limited to the high-p_T region of the spectrum, and do not include small-p_T resummation. Also our study is the first to include the analytic resummation rather that the parton shower. In this contribution we present the resummed p_T-spectrum at NLO+NLL accuracy, with the inclusion of a set of dimension-six parameters relevant for Higgs boson production.

3. Effective operators and their impact on the Higgs production cross section

We consider the effective Lagrangian

$$\mathcal{L} = \mathcal{L}_{SM} + \sum_i \frac{c_i}{\Lambda^2}\mathcal{O}_i \tag{2}$$

where the SM is supplemented by the inclusion of a set of dimension-six operators describing new physics effects at a scale Λ well above the electroweak scale. In our study we consider the following four operators

$$\mathcal{O}_1 = |H|^2 G^a_{\mu\nu} G^{a,\mu\nu}\,, \quad \mathcal{O}_2 = |H|^2 \bar{Q}_L H^c u_R + h.c.\,, \tag{3}$$

$$\mathcal{O}_3 = |H|^2 \bar{Q}_L H d_R + h.c.\,, \quad \mathcal{O}_4 = \bar{Q}_L H \sigma^{\mu\nu} T^a u_R G^a_{\mu\nu} + h.c. \tag{4}$$

These operators, in the case of single Higgs production, may be expanded as:

$$\frac{c_1}{\Lambda^2}\,\mathcal{O}_1 \to \frac{\alpha_S}{\pi v} c_g h G^a_{\mu\nu} G^{a,\mu\nu}\,, \tag{5}$$

$$\frac{c_2}{\Lambda^2}\,\mathcal{O}_2 \to \frac{m_t}{v} c_t h \bar{t}t\,, \tag{6}$$

$$\frac{c_3}{\Lambda^2}\,\mathcal{O}_3 \to \frac{m_b}{v} c_b h \bar{b}b\,, \tag{7}$$

$$\frac{c_4}{\Lambda^2}\,\mathcal{O}_4 \to c_{tg}\frac{g_S m_t}{2v^3}(v+h) G^a_{\mu\nu}(\bar{t}_L \sigma^{\mu\nu} T^a t_R + h.c)\,. \tag{8}$$

The operator $\mathcal{O}_1$ corresponds to a contact interaction between the Higgs boson and gluons with the same structure as in the heavy-top limit (HTL) of the SM. The operators $\mathcal{O}_2$ and $\mathcal{O}_3$ describe modifications of the top and bottom Yukawa couplings. The operator $\mathcal{O}_4$ is the chromomagnetic dipole-moment operator, which modifies the interactions between the gluons and the top quark[2] (here $\sigma^{\mu\nu} = \frac{i}{2}[\gamma^\mu, \gamma^\nu]$). In our convention, based on the SILH basis [34, 35], we express the Wilson coefficients as factors in the canonically normalized Lagrangian.

The coefficients c_t, c_b and c_g can be probed in Higgs boson processes. In particular, c_t (and c_b) may be measured in the $t\bar{t}H$ (and $b\bar{b}H$) production modes.The coefficient c_b can also be accessed through the decay $H \to b\bar{b}$. The coefficient c_{tg}, instead, is constrained by top pair production [36].

We now consider the contribution of the effective operators $\mathcal{O}_1, \mathcal{O}_2$ and $\mathcal{O}_4$ on the production cross section, while omitting, for simplicity, the bottom contribution in $\mathcal{O}_3$. The relevant Feynman diagrams are displayed in Fig. 1. The corresponding amplitude can be cast into the form

$$\mathcal{M}\left(g(p_1) + g(p_2) \to H\right) = i\frac{\alpha_S}{3\pi v}\epsilon_{1\mu}\epsilon_{2\nu}\left[p_1^\nu p_2^\mu - (p_1 p_2) g^{\mu\nu}\right] F(\tau)\,, \tag{9}$$

where $\tau = 4m_t^2/m_h^2$ and ϵ_1 and ϵ_2 are the polarization vectors of the incoming gluons. The contribution of the chromomagnetic operator to the function $F(\tau)$ has been addressed in the literature with contradicting results [37, 38] (see also Ref. [39]). In Ref. [37] it is found that the UV divergences in the bubble and triangle contributions cancel out. In the revised version of

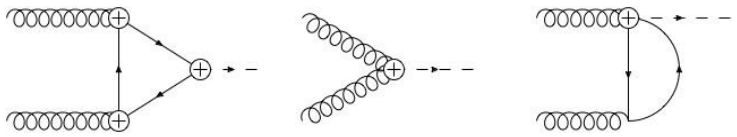

Figure 1. Feynman diagrams contributing to $gg \to H$ production at LO. The possible insertions of dimension-six operators are marked by a cross in a circle.

Ref. [38] it is instead stated that the UV divergence is present, and it has to be reabsorbed into the coefficient c_g.

Our results are consistent with the latter statement. We find

$$F(\tau) = \Gamma(1+\epsilon)\left(\frac{4\pi\mu^2}{m_t^2}\right)^{\epsilon}\left(c_t F_1(\tau) + c_{g0}F_2(\tau) + Re(c_{tg})\frac{m_t^2}{v^2}F_{30}(\tau)\right), \tag{10}$$

where

$$F_1(\tau) = \frac{3}{2}\tau\left[1 + (1-\tau)f(\tau)\right], \tag{11}$$

$$F_2(\tau) = 12, \tag{12}$$

$$F_{30}(\tau) = \frac{6}{\epsilon} + 3\left[1 - \tau f(\tau) - 2g(\tau)\right], \tag{13}$$

with the functions

$$f(\tau) = \begin{cases} \arcsin^2\dfrac{1}{\sqrt{\tau}} & \tau \geq 1 \\ -\dfrac{1}{4}\left[\ln\dfrac{1+\sqrt{1-\tau}}{1-\sqrt{1-\tau}} - i\pi\right]^2 & \tau < 1 \end{cases}. \tag{14}$$

$$g(\tau) = \begin{cases} \sqrt{\tau-1}\arcsin\dfrac{1}{\sqrt{\tau}} & \tau \geq 1 \\ \sqrt{1-\tau}\left[\ln\dfrac{1+\sqrt{1-\tau}}{1-\sqrt{1-\tau}} - i\pi\right] & \tau < 1 \end{cases}. \tag{15}$$

The $1/\epsilon$ divergence can be reabsorbed in the $\overline{\text{MS}}$ renormalization of the coefficient c_g:

$$c_{g0} = c_g(\mu_R) + \delta c_g \tag{16}$$

with

$$\delta c_g = \frac{m_t^2}{2v^2}Re(c_{tg})\Gamma(1+\epsilon)(4\pi)^{\epsilon}\left(-\frac{1}{\epsilon} - \ln\frac{\mu^2}{\mu_R^2}\right), \tag{17}$$

where μ_R denotes the renormalization scale of c_g. The final result reads

$$F(\tau) = c_t F_1(\tau) + c_g(\mu_R)F_2(\tau) + Re(c_{tg})\frac{m_t^2}{v^2}F_3(\tau), \tag{18}$$

where

$$F_3(\tau) = 3\left(1 - \tau f(\tau) - 2g(\tau) + 2\ln\frac{\mu_R^2}{m_t^2}\right). \tag{19}$$

[2] In this analysis we do not consider the contribution of the chromomagnetic dipole operator of the bottom quark.

In the HTL $m_t^2 \gg m_h^2$ we have

$$F_1(\tau) \to 1\,, \qquad F_2(\tau) \to 12\,, \qquad F_3(\tau) \to 6\left(\ln\frac{\mu_R^2}{m_t^2} - 1\right)\,. \tag{20}$$

In the SM we have $c_t = 1$ and $c_g = c_{tg} = 0$, so that $F(\tau) \to F_1(\tau)$. In Ref. [36] data on top production are used to extract constraints on c_{tg}. The resulting region of allowed values of c_{tg} has been found to be

$$-0.04 \lesssim c_{tg} \lesssim 0.04\,. \tag{21}$$

The impact on the total cross section is less than 20%. We conclude that, although smaller than the impact of c_g, the effect of c_{tg} can still be important. We note, however, that the chromomagnetic operator provides a contribution which is formally $\mathcal{O}(\lambda_t^2)$ with respect to the others. In a strict expansion in α_S it can be neglected. This is what we will do in the next Section.
Focusing on the impact of c_t and c_g, we note that the total cross section alone does not allow us to disentangle the coefficients c_g and c_t:

$$\sigma \approx |12c_g + c_t|^2\sigma_{SM} \quad (HTL)\,. \tag{22}$$

As already noted in the literature [29], the transverse momentum spectrum allows us to break this degeneracy.

4. Results

In this section we present the p_T spectra of Higgs particle, including the modification coming from the effective operators. As the reference the NLO+NLL SM predictions are also showed on the Figures, with the grey band on the lower panel showing the perturbative uncertainty. The uncertainties of the renormalization and factorization scales are estimated by performing the customary seven-point μ_R, μ_F variation, i. e. we consider independent variations within the range $\mu_0/2 \leq \mu_F, \mu_R \leq 2\mu_0$ with $1/2 < \mu_R/\mu_F < 2$, where $\mu_0 = \sqrt{p_T^2 + m_H^2}/2$. We then vary also three resummation scales by a factor of two. [3] It results in the uncertainty of about $\pm 20\%$ at the peak, to about $+50\%$ -30% at $p_T = 400$ GeV. The values chosen for the effective coupling were guided by the (generalisation) of (22), to obtain the total cross section within 20% of SM value, what is the current experimental bound [4].

We start our analysis by considering the individual contribution of exactly one operator. Looking at the low-p_T interval (0 GeV$\leq p_T \leq$ 400 GeV) in Fig. 2 (a) we can directly deduce that modifications of the bottom Yukawa coupling through c_b dominantly affect the low-p_T shape of the distribution. In fact, at very low p_T we find effects that can even exceed the uncertainty of the SM prediction. As expected, $c_b < 1$ ($c_b > 1$) softens (hardens) the spectrum in that region.[5] The point-like Higgs-gluon coupling c_g, on the other hand, modifies the p_T-shape most notably at large transverse momenta (400 GeV$\leq p_T \leq$ 800 GeV), see Fig. 2 (b), where a positive (negative) c_g value hardens (softens) the spectrum. As expected, modifications of solely the top Yukawa through c_t have almost exclusively the effect of a rescaling of the total cross section. The deviations from the SM prediction through the dimension-six operators are within the scale uncertainty, although the differences in shape give some additional sensitivity to distinguish such effects. It is clear that in order to disentangle effects of this order it is necessary to start from a more accurate SM prediction.

[3] For the details of the calculation set up see our paper [1].
[4] Note that variations of the p_T distributions can be much larger due to the large experimental uncertainties.
[5] We point out, however, that this is true only when small deviations of c_b from its SM value $c_b = 1$ are considered. In this case the dominant effect of c_b is on the top-bottom interference. When c_b is significantly different from unity the squared bottom-loop contribution can change the picture.

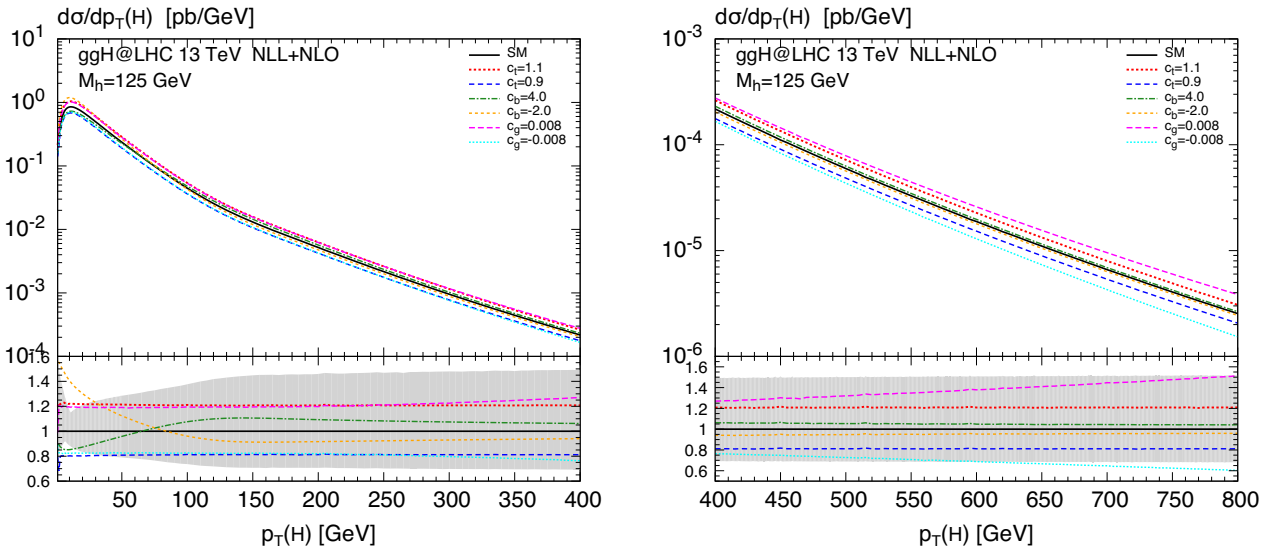

(a) (b)

Figure 2. Higgs transverse-momentum spectrum in the SM (black, solid) compared to separate variations of the dimension-six operators for (a) 0 GeV$\leq p_T \leq$ 400 GeV and (b) 400 GeV$\leq p_T \leq$ 800 GeV. The lower frame shows the ratio with respect to the SM prediction. The shaded band in the ratio indicates the uncertainty due to scale variations. See text for more details.

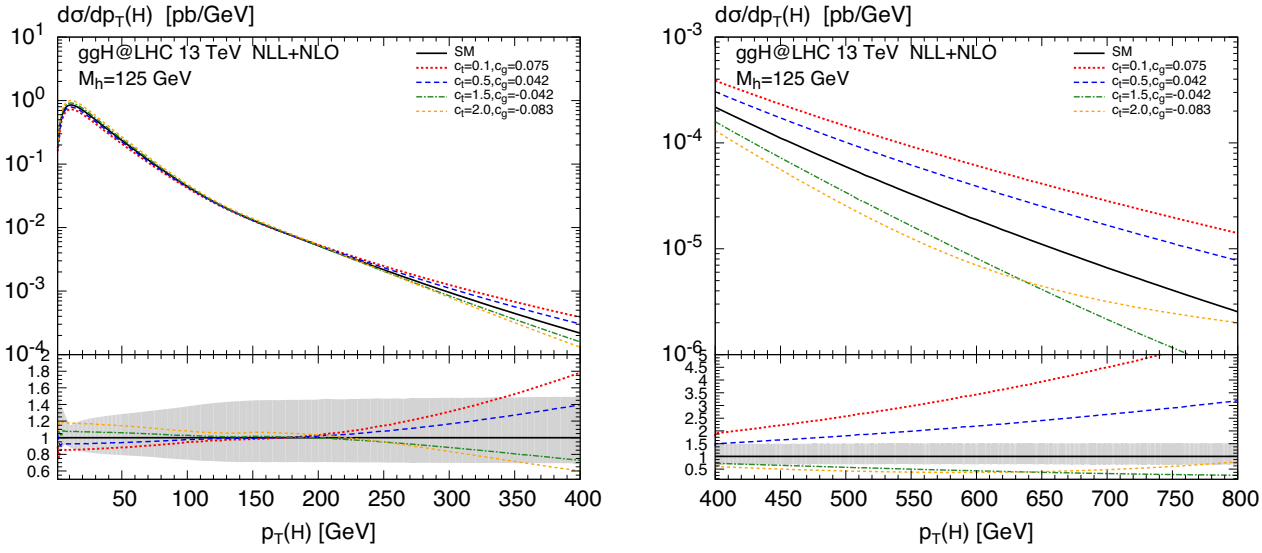

(a) (b)

Figure 3. Higgs transverse-momentum spectrum in the SM (black, solid) compared to simultaneous variations of c_t and c_g for (a) 0 GeV$\leq p_T \leq$ 400 GeV and (b) 400 GeV$\leq p_T \leq$ 800 GeV. The lower frame shows the ratio with respect to the SM prediction. The shaded band in the ratio indicates the uncertainty due to scale variations. See text for more details.

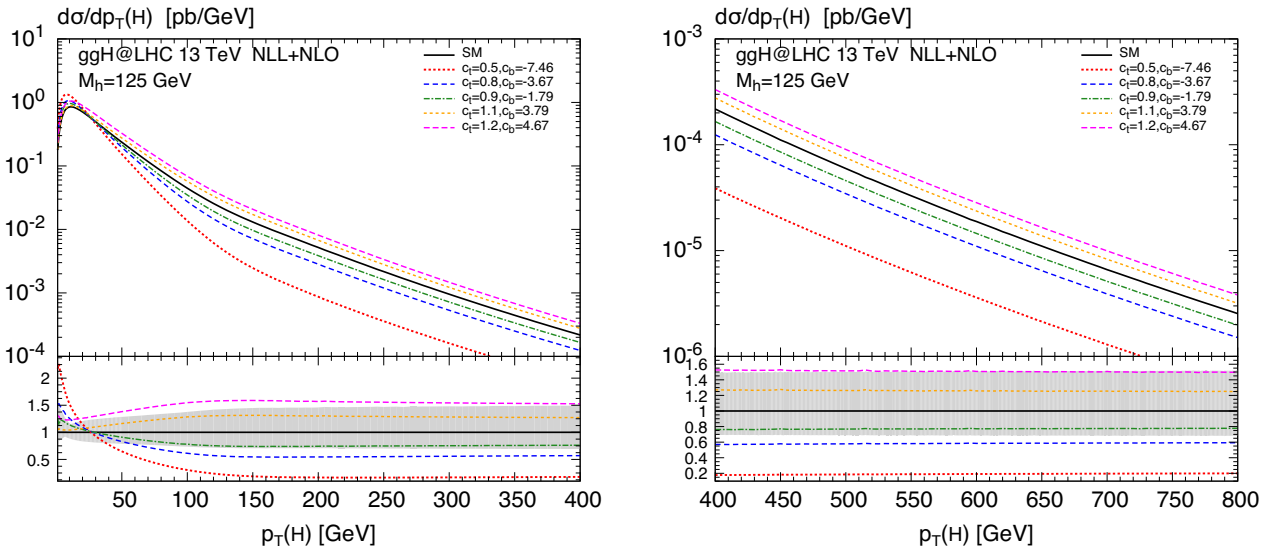

(a) (b)

Figure 4. Higgs transverse-momentum spectrum in the SM (black, solid) compared to simultaneous variations of c_t and c_b for (a) 0 GeV$\leq p_T \leq$ 400 GeV and (b) 400 GeV$\leq p_T \leq$ 800 GeV. The lower frame shows the ratio with respect to the SM prediction. The shaded band in the ratio indicates the uncertainty due to scale variations. See text for more details.

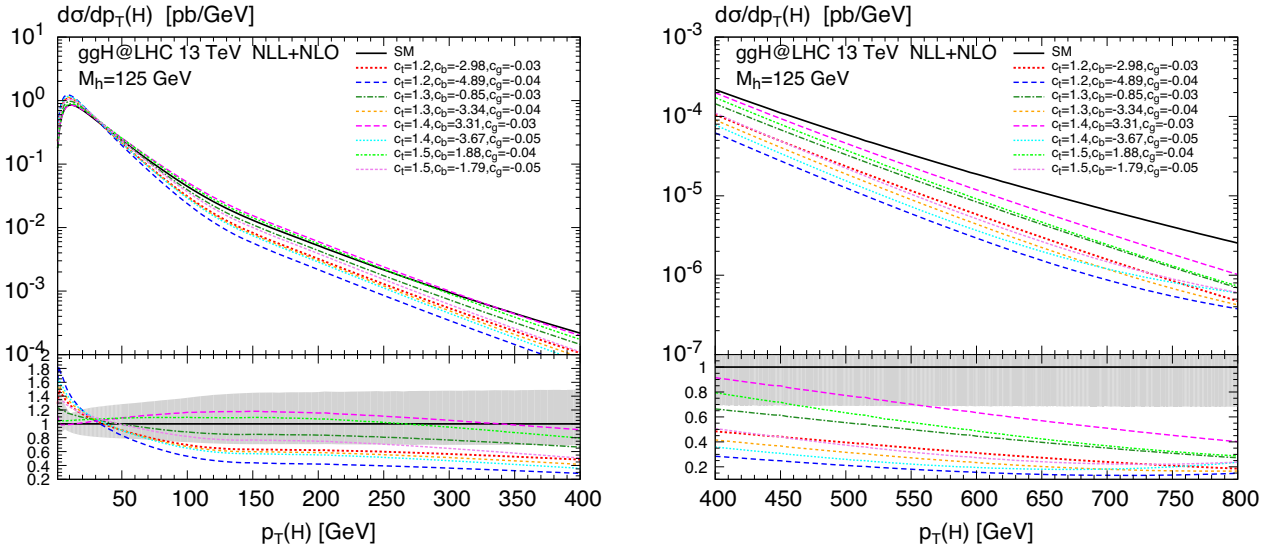

(a) (b)

Figure 5. Higgs transverse-momentum spectrum in the SM (black, solid) compared to simultaneous variations of c_t, c_g and c_b for (a) 0 GeV$\leq p_T \leq$ 400 GeV and (b) 400 GeV$\leq p_T \leq$ 800 GeV. The lower frame shows the ratio with respect to the SM prediction. The shaded band in the ratio indicates the uncertainty due to scale variations. See text for more details.

By contrast, the simultaneous variation of more than a single coefficient, as considered in Figs. 3-5, gives rise to more significant effects. The c_g, c_t and c_b parameters are chosen in the ballpark suggested by the studies of Refs. [6, 7, 8], while still keeping the inclusive cross section within about 20% of its SM value. Indeed, many combinations of c_g, c_t and c_b can be found which mildly affect the total cross section, while significantly changing the shape of the spectrum.

In Fig. 3 we present the simultaneous variation of c_t and c_g. In this case, both the small and high-p_T behaviour of the spectrum is altered by the different combinations of c_t and c_g coefficients. It is clear that in particular the large-p_T region offers a good discrimination between the different structures of c_t and c_g in terms of shape. Again, negative (positive) c_g values will soften (harden) the spectrum. The effects are well beyond the theoretical uncertainties already at NLL+NLO. We note that the yellow, short-dashed curve corresponding to $c_t = 2$, $c_g = -0.083$ develops a minimum in the ratio to the SM around $\sim 650\,\text{GeV}$. This is due to a compensation between the negative interference between the $\mathcal{O}_1$ and $\mathcal{O}_2$ operators, which is proportional to $c_g c_t$ and the contribution of $\mathcal{O}_1$ itself, which is proportional to c_g^2 and tends to produce a harder spectrum with respect to the SM prediction.

Fig. 4 shows spectra with modified top and bottom Yukawa couplings. In this case, the compensation of the BSM contributions is less straightforward, and it is difficult to compensate $c_t > 1$ without significantly affecting the inclusive cross section. For the magenta, long-dashed curve ($c_t = 1.2$, $c_b = 4.67$) we, thus, allow for a bigger change of the total cross section up to 30%. As pointed out before, the bottom-loop softens the spectrum and, since the variation of the bottom Yukawa coupling is rather large, the squared bottom-term is larger than the top-bottom interference term and the spectrum is softened also when negative c_b values are considered. The shape difference to the SM is very significant, but only in the small-p_T region, where the soft-gluon resummation is crucial to obtain a reliable prediction. Indeed, the contribution of the bottom loop decreases with growing p_T [40] and above 150 GeV the spectra have all very similar shapes with c_t driving their normalisation.

Finally, we discuss spectra obtained by switching on all three SMEFT operators, as shown in Fig. 5. Our focus here is on scenarios with increased top-quark Yukawa coupling (up to $c_t = 1.5$). These scenarios would be of particular interest in the case in which the excess on the $t\bar{t}H$ rate over the SM prediction [41, 42] should be confirmed. In order to compensate the increase in the cross section driven by $c_t > 1$ a negative c_g has been chosen. We observe a general tendency of the BSM spectra to fall below the SM prediction in the intermediate and high transverse-momentum regions, which is due to the negative c_g contribution. The total rate is compensated by the enhancement in the low p_T region, due to a combination of the negative c_g coefficient with both negative and positive c_b modifications. Overall, we find sizeable distortions of the p_T shapes due to the dimension-six operators far beyond the scale uncertainties of the NLL+NLO SM prediction, that exceed the previously considered scenarios with two simultaneous varied coefficients in both size and significance. Despite the similar overall behaviour, the predictions for the various scenarios may differ significantly, which enables their discrimination when compared to data.

We conclude this Section with a comment on the validity of the EFT approach. The computation we have performed is carried out under the assumption that we can consider the effects of higher-dimensional operators as a "small" perturbation with respect to the SM result. This implies in particular that the effect of dimension-eight operators can be neglected. This is not obvious, given that we are studying also the large transverse-momentum region. To check the above assumption we have repeated our calculations by dropping the $\mathcal{O}(1/\Lambda^4)$ suppressed terms originating from the square of the dimension-six contributions. We find that in most of the cases the differences with respect to the results shown in Figs. 2-5 are very small, even at high transverse momenta. Only in the scenarios considered in Fig. 3 ($c_t = 0.1, c_g = 0.075$ and $c_t = 2, c_g = -0.083$) the $\mathcal{O}(1/\Lambda^4)$ effects are important, and thus, the corresponding quantitative

results should be interpreted with care.

5. Conclusions

New Physics might be not accessible at the LHC through direct searches, e.g., with the discovery of new resonances. In that case, it is crucial to fully exploit the data to study possible (small) deviations from the SM predictions. SMEFT offers a formalism for the parametrisation of high-scale BSM effects, which can be used for this purpose. In the SMEFT framework BSM effects are parametrised through appropriate higher-dimensional operators, and bounds on the corresponding Wilson coefficients can be set by comparing to the experimental data.

In this paper, we have presented a computation of the transverse-momentum spectrum of the Higgs boson in which the SM prediction is supplemented by possible BSM effects. Such effects are modeled by augmenting the SM Lagrangian with appropriate dimension-six operators. Our calculation consistently includes all the terms up to $\mathcal{O}(\alpha_S^3)$ accuracy and is supplemented by soft-gluon resummation at NLL accuracy, which is required to obtain reliable predictions at small transverse momenta. At the same level of accuracy we implement three dimension-six operators, related to the modifications of top and bottom Yukawa couplings and to the inclusion of a point-like ggH coupling. Additionally, we studied the impact of the chromomagnetic operator on the Higgs cross section at LO.

We have constructed a tool for reliable predictions of the Higgs p_T distribution including dimension-six operators and performed a comprehensive study of the possible effects due to the different dimension-six operators. We varied the c_t, c_b and c_g coefficients in the range suggested by recent global analyses and required the total cross section to meet the SM prediction at NLO within the current $\mathcal{O}(20\%)$ experimental uncertainty.

We found that variations of different SMEFT operators manifest themselves in different regions of the Higgs p_T spectrum:

- a modification of the Higgs-bottom Yukawa coupling ($\mathcal{O}_3$) induces effects almost exclusively at small transverse momenta
- a direct coupling of the Higgs boson to gluons ($\mathcal{O}_1$) changes the shape of the distribution in the high-p_T tail
- a change in the top-quark Yukawa coupling ($\mathcal{O}_2$) primarily affect the normalisation of the spectrum.

We can notice, from the presented spectra, that the shape of the transverse momentum distribution depends on the mass of the particle that mediates the Higgs-gluon coupling. The lower the mass of that particle, the softer is the resulting spectrum, and thus the enhancement of bottom loop leads to the softest spectra, while enhancement of point-like coupling (corresponding to infinite mass particle in the loop) to the hardest one.

To finalise our conclusions we mention the limitations of our study. Although with simultaneous contributions of the effective operators the spectra can easily exceed the uncertainties of NLL+NLO SM prediction, this is not the case for the separate operator's contribution. This calls for the increase of the precision of the calculations. The NNLL+NNLO predictions for the SM are known, however only on in the HTL approximation. Nonetheless, the relative BSM/SM effects we have obtained in this paper (i.e., the ratios plotted in the lower panels of Figs. 2-5) can be used to include BSM effects on top of NNLL+NNLO accurate SM predictions.

Another aspect which deserves some comments is the set of dimension-six operators we have considered. In the present calculation we have limited ourselves to consider the contributions of the operators related to modified top and bottom Yukawa couplings and of the additional direct Hgg interaction. As discussed in Sec. 3, although formally suppressed by two powers of the top Yukawa coupling, the chromomagnetic operator could still significantly contribute, within the

current bounds on its Wilson coefficient, to the gluon fusion cross section. The extension of our calculation to include these effects is left for future work.

Acknowledgments
I would like to thank prof. Krawczyk for the invitation to the Discrete conference and acknowledge the financial support from the HARMONIA project under contract UMO-2015/18/M/ST2/00518 (2016-2019). This work is supported by the 7th Framework Programme of the European Commission through the Initial Training Network HiggsTools PITN-GA-2012-316704.

References

[1] Grazzini M, Ilnicka A, Spira M and Wiesemann M 2016 (*Preprint* 1612.00283)
[2] Aad G *et al.* (ATLAS) 2013 *Phys. Lett.* **B716** 1–29 (*Preprint* 1207.7214)
[3] Chatrchyan S *et al.* (CMS) 2013 *Phys. Lett.* **B716** 30–61 (*Preprint* 1207.7235)
[4] Buchmuller W and Wyler D 1986 *Nucl. Phys.* **B268** 621–653
[5] Grzadkowski B, Iskrzynski M, Misiak M and Rosiek J 2010 *JHEP* **10** 085 (*Preprint* 1008.4884)
[6] Dumont B, Fichet S and von Gersdorff G 2013 *JHEP* **07** 065 (*Preprint* 1304.3369)
[7] Falkowski A 2016 *Pramana* **87** 39 (*Preprint* 1505.00046)
[8] Butter A, boli O J P, Gonzalez-Fraile J, Gonzalez-Garcia M C, Plehn T and Rauch M 2016 *JHEP* **07** 152 (*Preprint* 1604.03105)
[9] Aad G *et al.* (ATLAS) 2014 *JHEP* **09** 112 (*Preprint* 1407.4222)
[10] Aad G *et al.* (ATLAS) 2014 *Phys. Lett.* **B738** 234–253 (*Preprint* 1408.3226)
[11] Chatrchyan S *et al.* (CMS) 2015 *arXiv:1508.07819* (*Preprint* 1508.07819)
[12] Georgi H M, Glashow S L, Machacek M E and Nanopoulos D V 1978 *Phys. Rev. Lett.* **40** 692
[13] Ellis R K, Hinchliffe I, Soldate M and van der Bij J J 1988 *Nucl. Phys.* **B297** 221
[14] Baur U and Glover E W N 1990 *Nucl. Phys.* **B339** 38–66
[15] Schmidt C R 1997 *Phys. Lett.* **B413** 391
[16] de Florian D, Grazzini M and Kunszt Z 1999 *Phys. Rev. Lett.* **82** 5209–5212 (*Preprint* hep-ph/9902483)
[17] Glosser C J and Schmidt C R 2002 *JHEP* **12** 016 (*Preprint* hep-ph/0209248)
[18] Ravindran V, Smith J and Van Neerven W L 2002 *Nucl. Phys.* **B634** 247–290 (*Preprint* hep-ph/0201114)
[19] Harlander R V, Neumann T, Ozeren K J and Wiesemann M 2012 *JHEP* **08** 139 (*Preprint* 1206.0157)
[20] Neumann T and Wiesemann M 2014 *JHEP* **11** 150 (*Preprint* 1408.6836)
[21] Boughezal R, Caola F, Melnikov K, Petriello F and Schulze M 2013 *JHEP* **06** 072 (*Preprint* 1302.6216)
[22] Boughezal R, Caola F, Melnikov K, Petriello F and Schulze M 2015 *Phys. Rev. Lett.* **115** 082003 (*Preprint* 1504.07922)
[23] Chen X, Gehrmann T, Glover E W N and Jaquier M 2015 *Phys. Lett.* **B740** 147–150 (*Preprint* 1408.5325)
[24] Collins J C, Soper D E and Sterman G F 1985 *Nucl. Phys.* **B261** 104
[25] Bozzi G, Catani S, de Florian D and Grazzini M 2006 *Nucl. Phys.* **B737** 73–120 (*Preprint* hep-ph/0508068)
[26] Mantler H and Wiesemann M 2013 *Eur. Phys. J.* **C73** 2467 (*Preprint* 1210.8263)
[27] Grazzini M and Sargsyan H 2013 *JHEP* **09** 129 (*Preprint* 1306.4581)
[28] Grojean C, Salvioni E, Schlaffer M and Weiler A 2014 *JHEP* **05** 022 (*Preprint* 1312.3317)
[29] Azatov A and Paul A 2014 *JHEP* **01** 014 (*Preprint* 1309.5273)
[30] Langenegger U, Spira M and Strebel I 2015 *arXiv:1507.01373* (*Preprint* 1507.01373)
[31] Maltoni F, Vryonidou E and Zhang C 2016 *JHEP* **10** 123 (*Preprint* 1607.05330)
[32] Harlander R V and Neumann T 2013 *Phys. Rev.* **D88** 074015 (*Preprint* 1308.2225)
[33] Dawson S, Lewis I M and Zeng M 2014 *Phys. Rev.* **D90** 093007 (*Preprint* 1409.6299)
[34] Giudice G F, Grojean C, Pomarol A and Rattazzi R 2007 *JHEP* **06** 045 (*Preprint* hep-ph/0703164)
[35] Contino R, Ghezzi M, Grojean C, Muhlleitner M and Spira M 2013 *JHEP* **07** 035 (*Preprint* 1303.3876)
[36] Buarque Franzosi D and Zhang C 2015 *Phys. Rev.* **D91** 114010 (*Preprint* 1503.08841)
[37] Choudhury D and Saha P 2012 *JHEP* **08** 144 (*Preprint* 1201.4130)
[38] Degrande C, Gerard J M, Grojean C, Maltoni F and Servant G 2012 *JHEP* **07** 036 [Erratum: JHEP03,032(2013)] (*Preprint* 1205.1065)
[39] Chien Y T, Cirigliano V, Dekens W, de Vries J and Mereghetti E 2015 (*Preprint* 1510.00725)
[40] Langenegger U, Spira M, Starodumov A and Trueb P 2006 *JHEP* **06** 035 (*Preprint* hep-ph/0604156)
[41] Aad G *et al.* (ATLAS) 2016 (*Preprint* ATLAS-CONF-2016-080)
[42] Chatrchyan S *et al.* (CMS) 2016 (*Preprint* CMS-PAS-HIG-16-022)